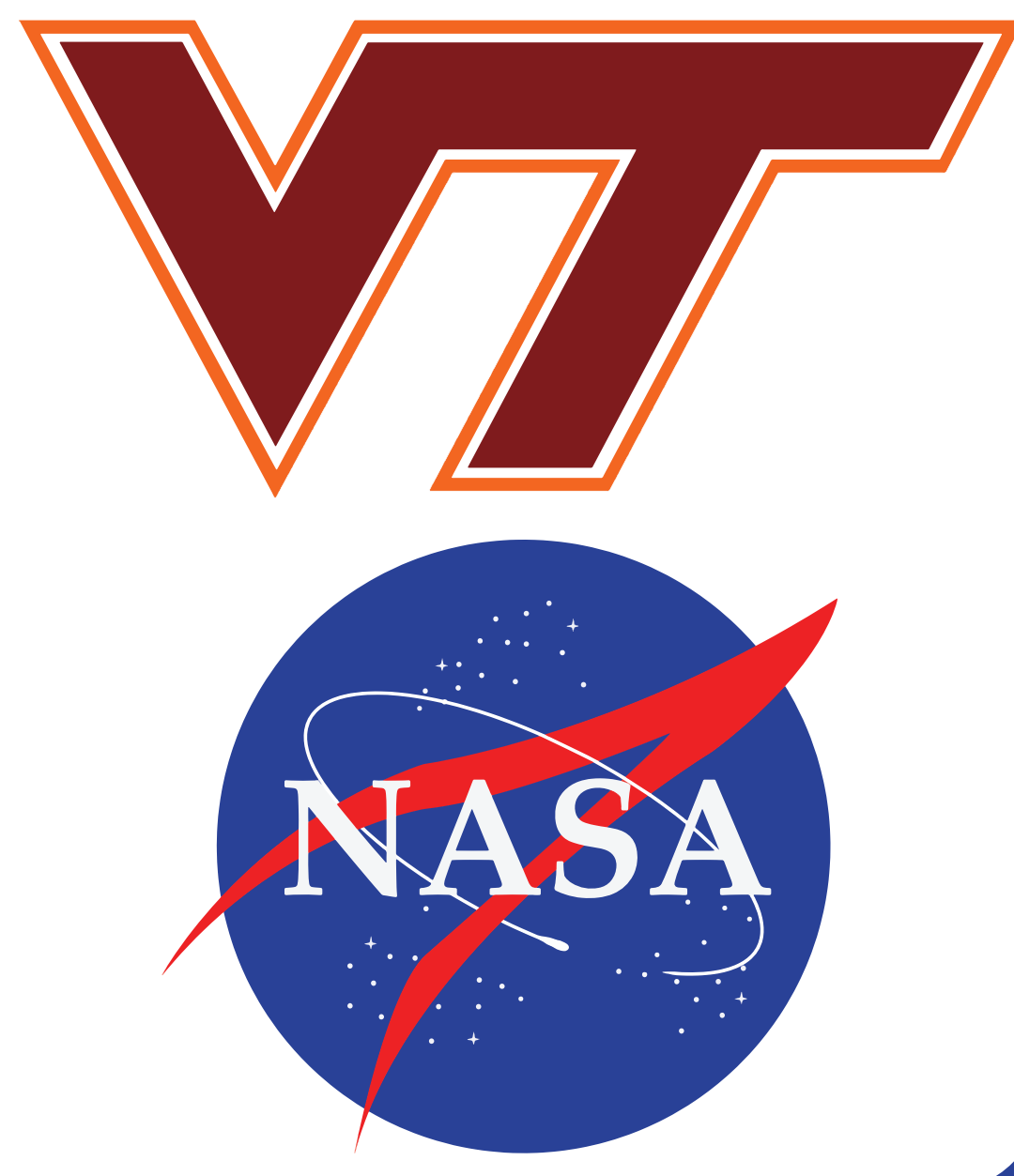


FORMATION OF A SHALLOW MAGMA OCEAN ON VESTA SUPPORTED BY MANTLE HARZBURGITE RESIDUA IN HOWARDITES

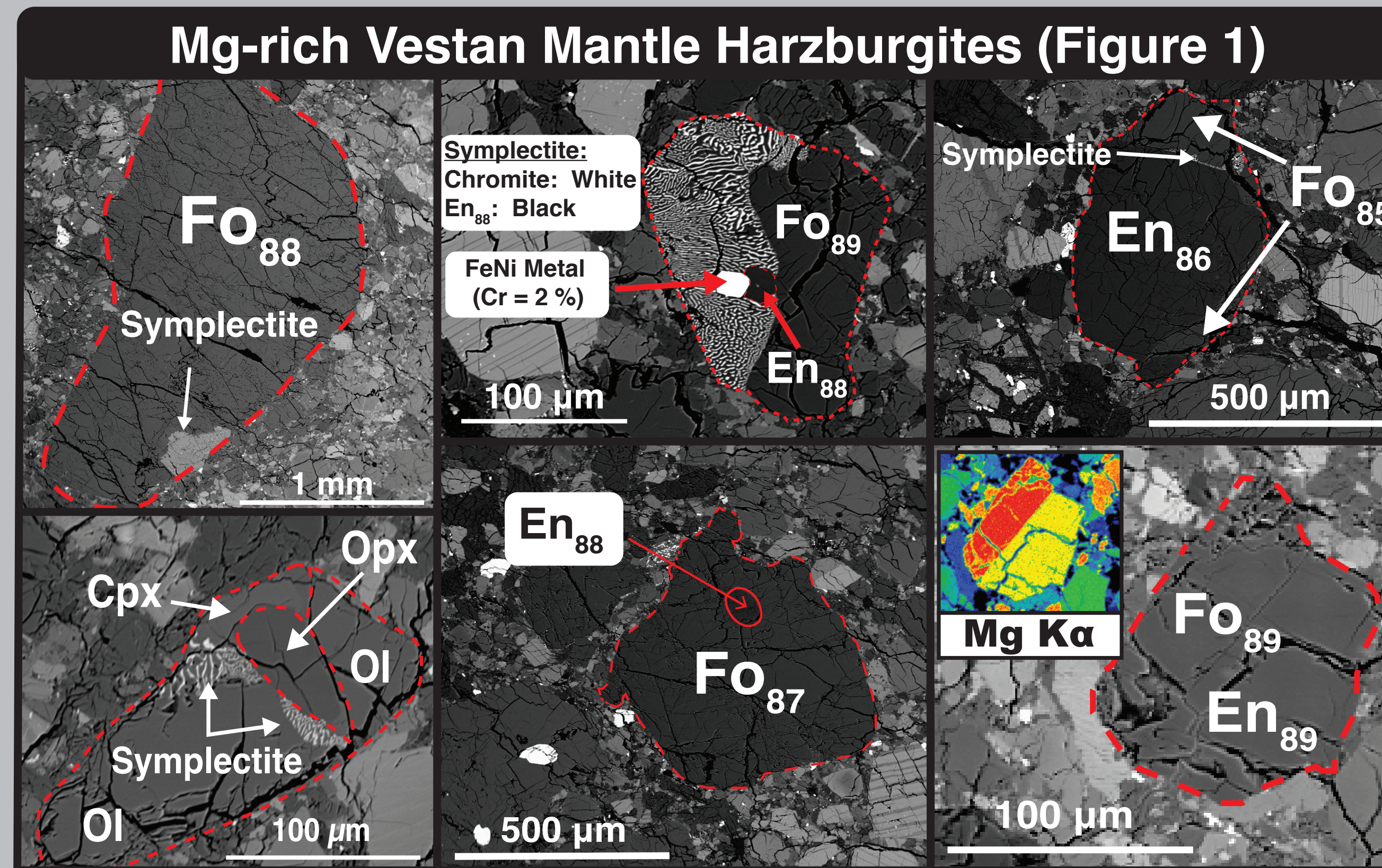


TIMOTHY M. HAHN JR.*, NICOLE G. LUNNING, HARRY Y. MCSWEEN, ROBERT J. BODNAR, AND LAWRENCE A. TAYLOR

*CORRESPONDENCE: DEPARTMENT OF EARTH AND PLANETARY SCIENCE, UNIVERSITY OF TENNESSEE, KNOXVILLE, TN 37996 (THAHN1@VOLS.UTK.EDU)

1) SUMMARY AND CONCLUSIONS:

- Mg-rich harzburgite clasts (Mg# 82-92) containing chromite-orthopyroxene symplectites occur in the Dominion Range 10 howardites.
- Olivine and pyroxene occur in textural and chemical equilibrium.
- Measured Fe/Mn consistent with a vestan origin.
- Major-element composition, high Ni/Co in olivines, and Cr in metal support a mantle origin for the harzburgite clasts.
- Fe/Mg and Fe/Mn systematics favor an origin as mantle residuum during incomplete melting, rather than cumulates from a magma ocean.
- Symplectite formation is hypothesized to represent the crystallization of a metasomatic melt, that altered the original trace-element composition of orthopyroxene, and was in disequilibrium with Mg-rich olivine – the metasomatic melt may represent trapped silicate and metallic melts during core formation and early differentiation.
- Geochemical modeling (MELTS) contradicts global magma ocean models, and instead suggests <50% melting below the IW buffer occurred, but that melting was sufficient enough to produce a Mg-rich residuum.

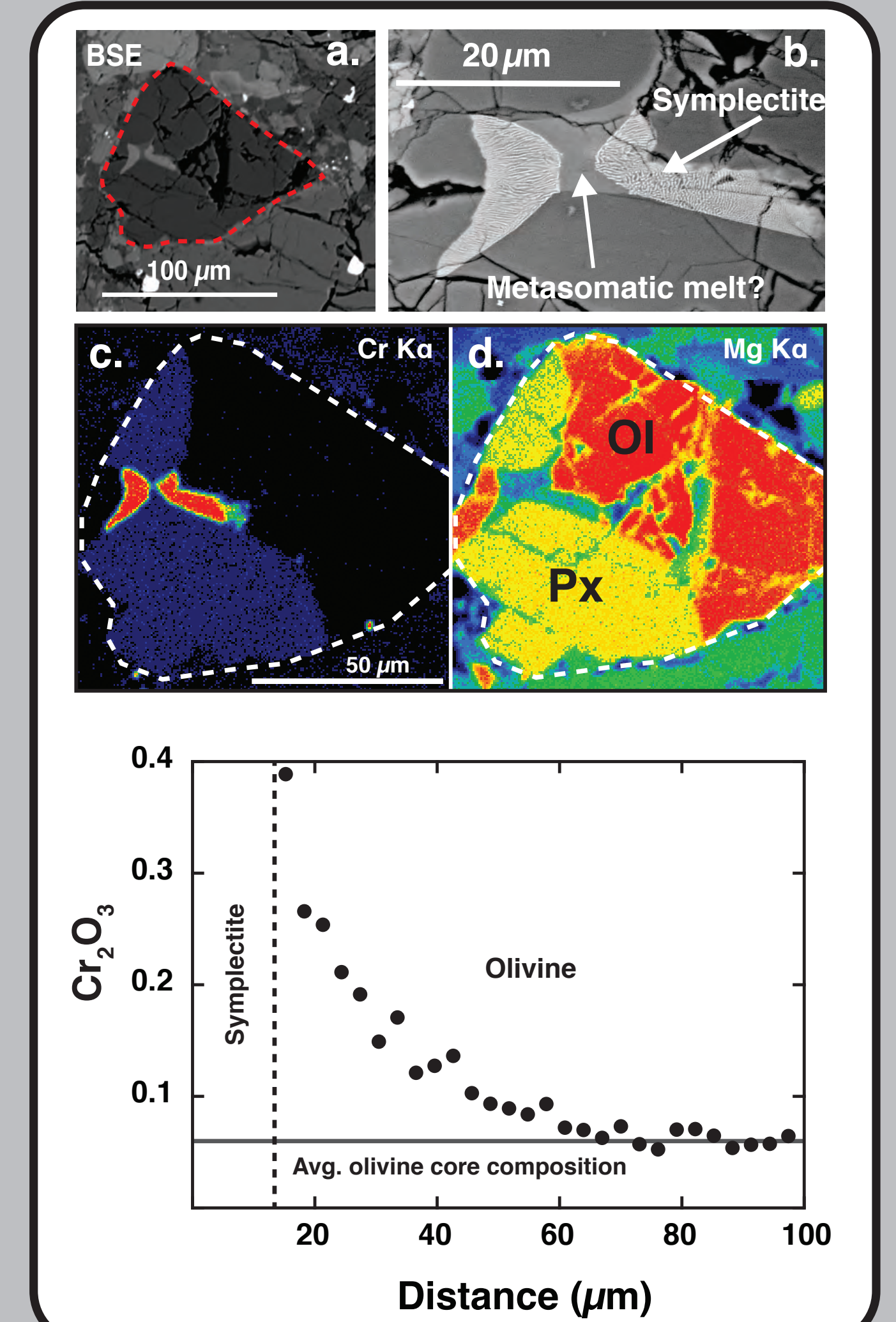
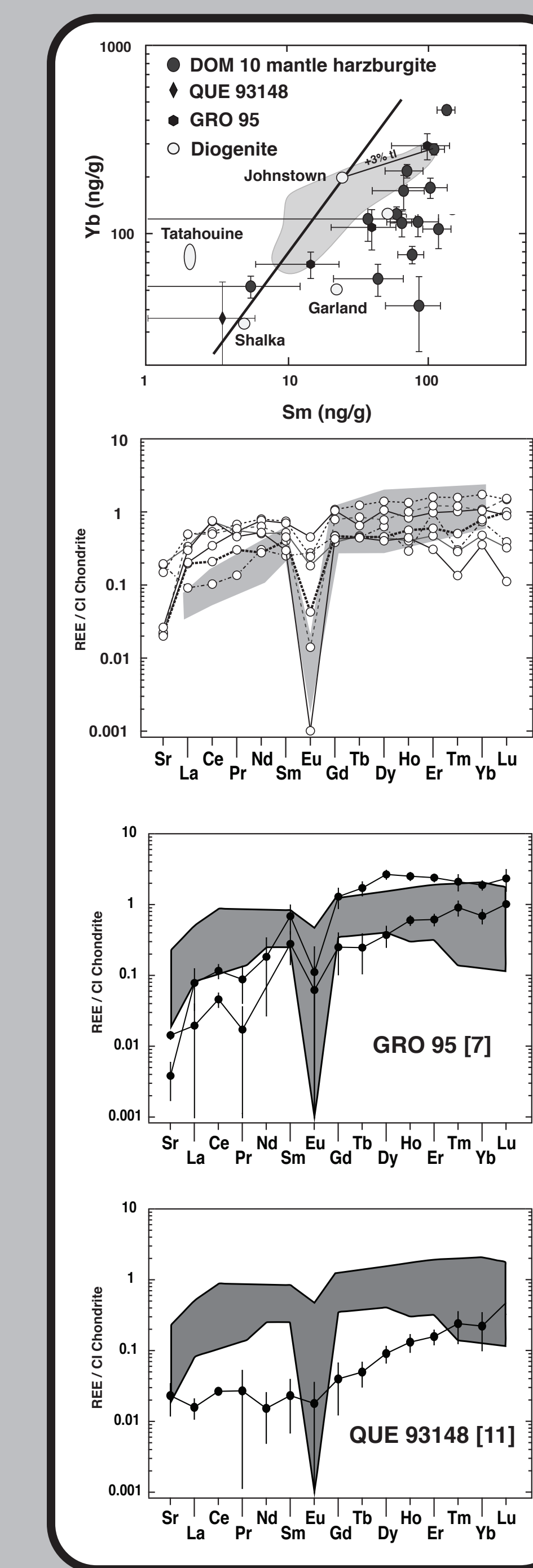
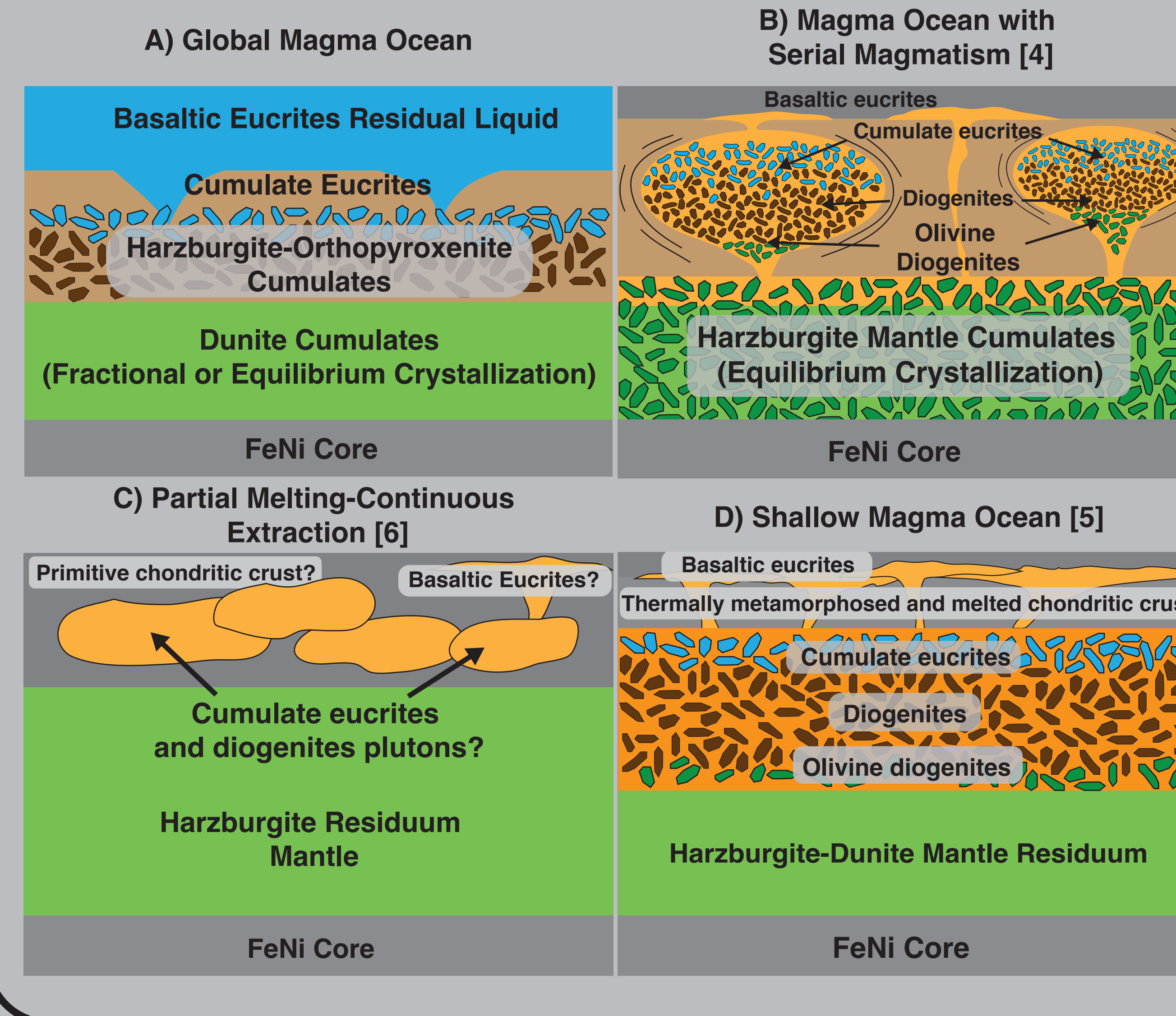


2) INTRODUCTION:

The differentiation of planetesimals in the early solar system is thought to be a common occurrence due to the decay of ²⁶Al [1]. These differentiated bodies were likely the building blocks for the terrestrial planets, and therefore the survival of such bodies (4 Vesta), provide unique opportunities to study their differentiation mechanisms and interior structures. The asteroid 4 Vesta has been extensively studied by the DAWN mission, and hundreds of associated howardite-eucrite-diogenite (HED) meteorites have been characterized [2].

Differentiation models of Vesta are commonly divided into two classes: partial melting with serial magmatism [3] and a global magma ocean [4]. Alternatively, models involving a shallow magma ocean [5] have been recently proposed, and are supported by physical constraints (i.e. melt ascent rates [6]). The mantles produced by different models vary in composition and physical setting; therefore, samples of the vestan mantle can provide a means to test these differentiation models [7,8]. Here we examine the major-, minor-, and trace-element chemistry of vestan harzburgite mantle clasts [8] in order to evaluate the petrogenesis of this lithology, and therefore provide constraints on the origin of the vestan mantle and the differentiation of Vesta.

Differentiation Models (Figure 6)



Figures 3 and 4:

Figure 3 (Left; Top to Bottom): (1) Trace-element composition of pyroxene in vestan mantle harzburgites; pyroxenes are enriched in LREE. (Modified from Mittlefehldt 1994). (2) REE patterns compared to typical diogenites [10]. (3) REE range of harzburgite clasts compared to Mg-rich olivine and pyroxene fragments in the GRO 95 howardites. (4) REE range of harzburgite clasts compared to QUE 93148, which is hypothesized to represent a mantle residuum. Figure 4 (Above): harzburgite clast with a possible trapped melt composition, which is reaction with olivine and pyroxene to produce the symplectite assemblage. Also, shown is the diffusion profile of Cr into olivine.

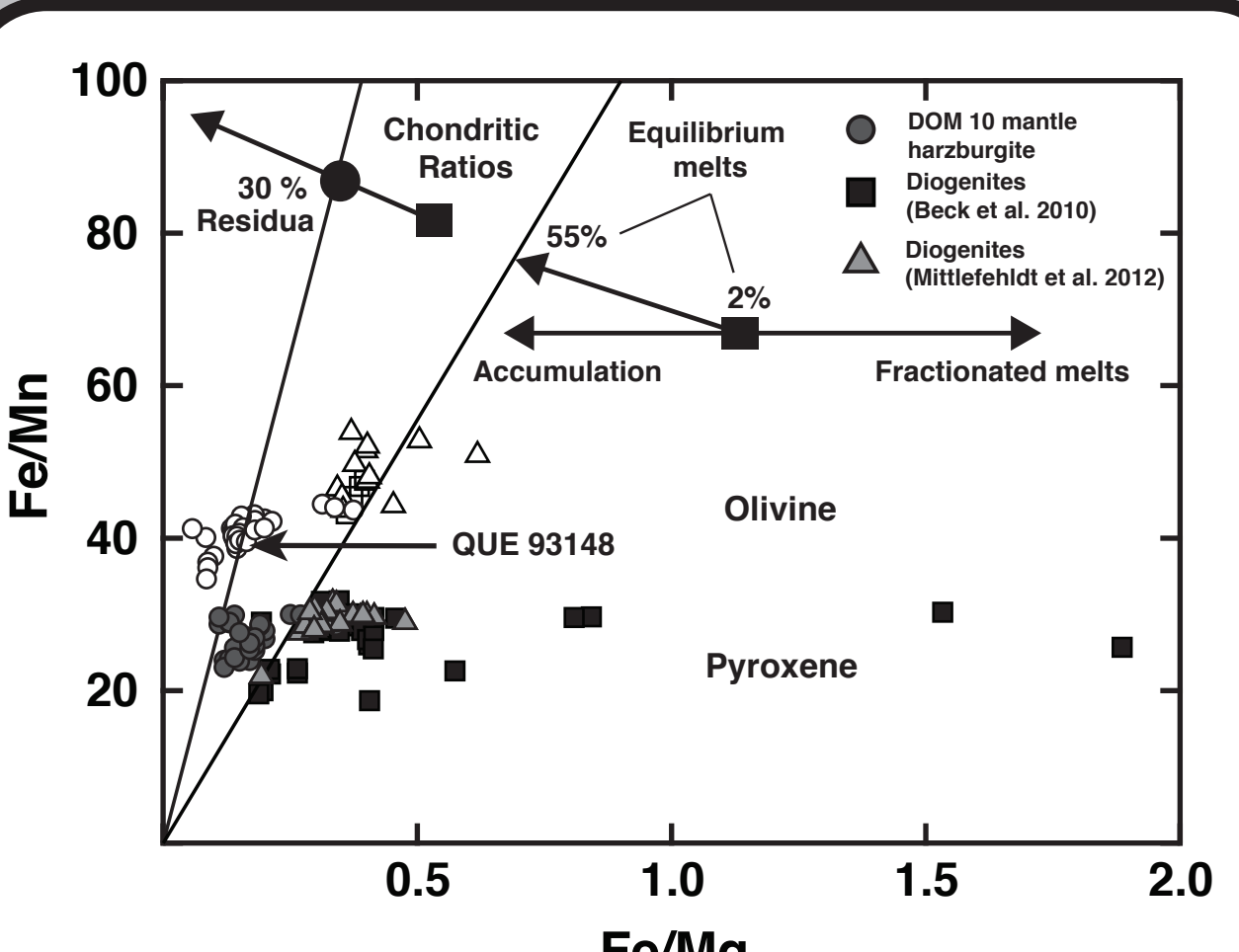
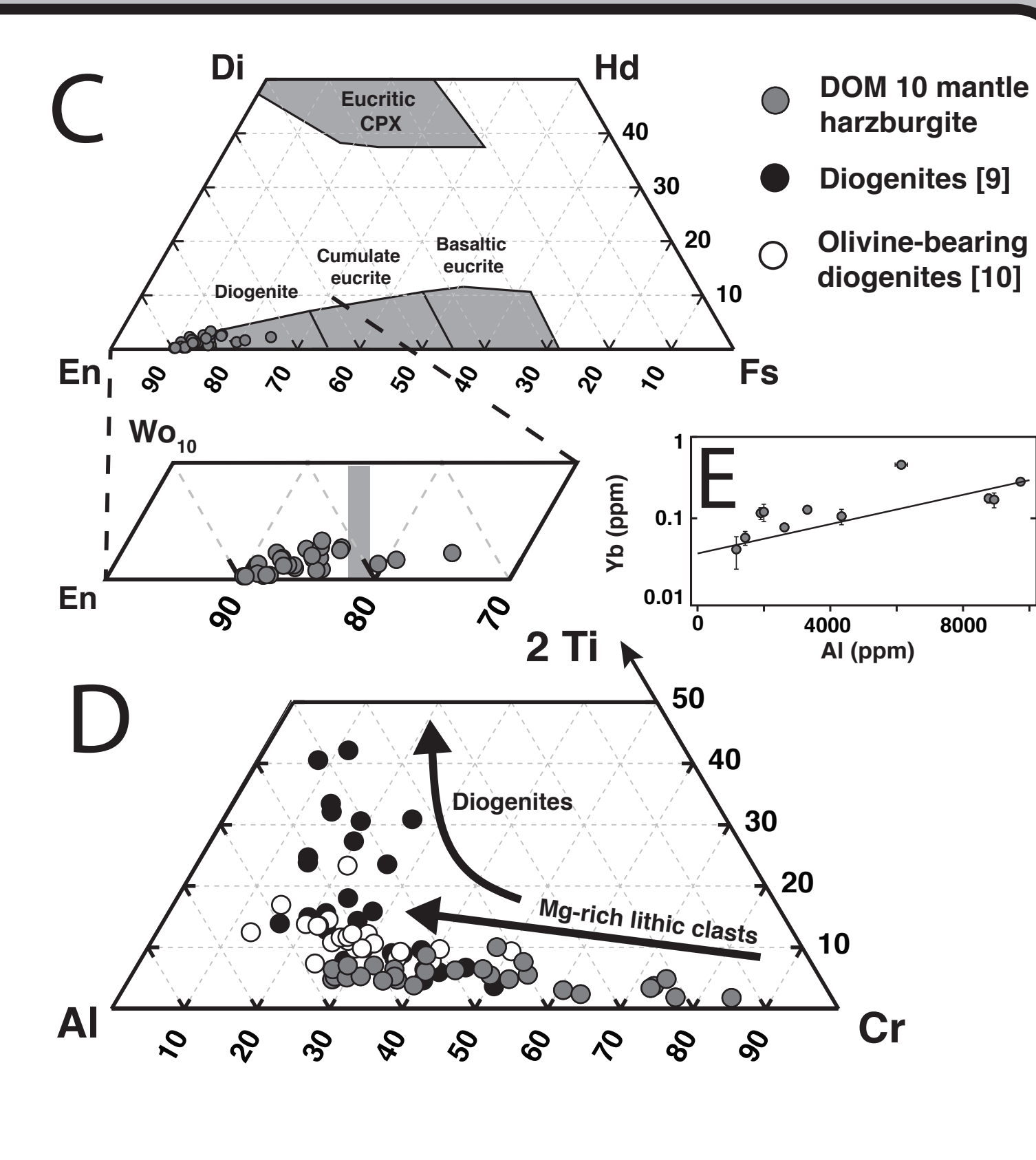
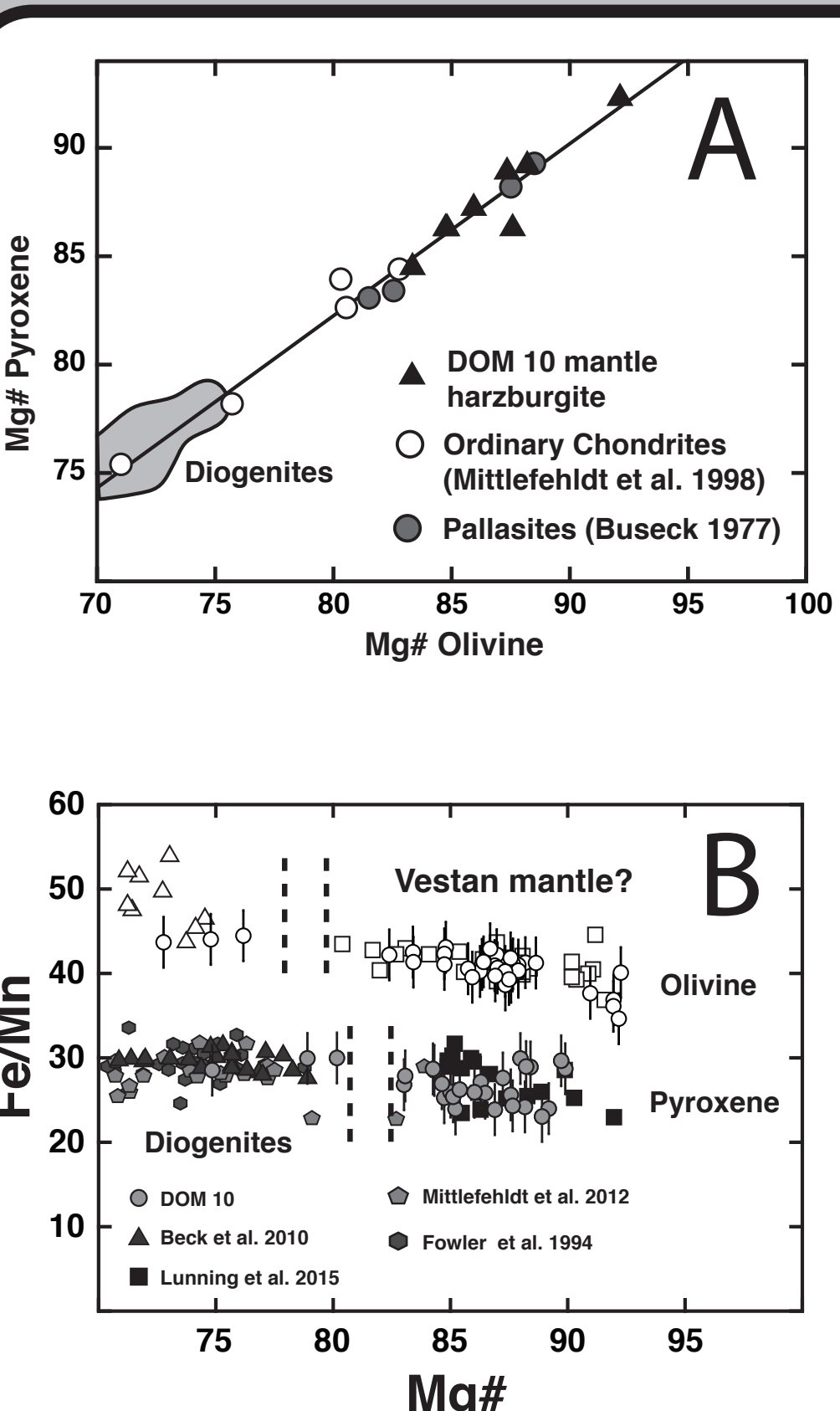


Figure 2: Above: (A) Co-existing olivine and pyroxene occur in equilibrium. (B) Fe/Mn plotted against Mg# for olivine and pyroxene; trends are consistent with a vestan origin, and a small compositional gap is apparent between Mg-rich harzburgite and diogenites. (C) Major-element composition of pyroxenes compared to typical HED lithologies. (D and E) Minor- and trace-element correlations suggest a common formation mechanism.

Figure 5: Left: Fe/Mn and Fe/Mg systematics for olivine and pyroxene in the harzburgite clasts. The trends exhibited by these minerals are inconsistent with accumulation and fractionation mechanisms, and suggests the harzburgite clasts are residua. For comparison, olivine and pyroxene from diogenites are shown.

3) RESULTS:

- Monomineralic, polycrystalline, and monomineralic polycrystalline lithic fragments of olivine and orthopyroxene occur in howardites (Figure 1).
- Olivine and pyroxene occur in chemical equilibrium and have Fe/Mn values consistent with Vesta, and Mg# 82-92 (Figure 2a-2c).
- Olivine has Ni and Co concentrations of 2 to 115 ppm and 9 to 43 ppm respectively.
- Minor-element correlations in orthopyroxene show an increasing Al/Cr with near-constant Ti (Figure 2d).
- Olivine trace-element concentrations below detection limits.
- Pyroxene is depleted relative to CI chondrites, and displays LREE enrichments not typical of orthopyroxene (Figure 3).
- Chromite-orthopyroxene symplectites associated with Mg-rich harzburgite clasts – adjacent olivines exhibit Cr diffusion profile (Figure 4)

4) DISCUSSION:

- Vestan mantle clasts show similarities to Mg-rich fragments in the GRO 95 howardites and QUE 93148; however, differences in trace-element concentrations are observed. We argue that these differences can be achieved by secondary processes. Specifically, interaction with a melt, which produced the symplectites, may have altered pyroxene trace-element composition.
- Symplectites in the mantle harzburgites resemble lunar symplectites [13]; textural characteristics imply crystallization from a trapped melt.
- Geochemical characteristics of harzburgite clasts (i.e. Fe/Mg and Fe/Mn systematics) indicate the clasts represent solid residua of the vestan mantle [14].
- The preservation of mantle residua in differentiation models places strict limitations on intensive properties (i.e. degree of melting). Specifically, mantle residuum is only observed with limited melting, although sufficient amounts of melting (>50%) are needed to produce a Mg-rich (Mg# >88) harzburgitic mantle. We interpret this to suggest that partial melting models are unlikely, and global magma ocean models do not preserve a mantle residuum. Our study, therefore, provides support for a shallow magma ocean.

5) IMPLICATIONS AND FUTURE WORK:

Our study supports the recently proposed shallow magma ocean differentiation model; however, the model proposed only considers physical parameters (i.e. melt density), and does not make compositional predictions of HED lithologies. Therefore, future work will now be aimed at developing a complementary geochemical model, while using the results of this study to constrain such models. Additionally, we intend to examine the chromite-orthopyroxene symplectites further, in order to understand their petrogenesis, and ultimately their implications for the formation of the vestan mantle. Specifically, future work will be aimed at experimental work on the potential trapped melt composition identified, and whether or not this melt composition can produce the symplectites through a reaction with Mg-rich olivines and/or pyroxene.

References: [1] Bizziro et al. (2005) *The Astrophysical Journal*, 632, 41-44. [2] McSween et al. (2013) *M.A.P.S.*, 48, 2090-2104. [3] Stolpher E. (1977) *G.C.A.*, 41, 587-611. [4] Mandler B.E. and Elkins-Tanton D.M. (2013) *M.A.P.S.*, 48, 2333-2349. [5] Neumann W. et al. (2014) *EPSL*, 393, 267-280. [6] Wilson T. and Kool J. (2012) *Chemical Earth*, 2, 289-321. [7] Lunning N.G. et al. (2015) *EPSL*, 418, 126-135. [8] Hahn T.M. et al. (2015) *Met. L.G.*, #1804. [9] Mittlefehldt D.W. et al. (2012) *M.A.P.S.*, 47, 72-78. [10] Fowlkes G.W. et al. (1994) *G.C.A.*, 58, 3921-3929. [11] Boss C. (2002) *M.A.P.S.*, 37, 1129-1139. [12] Toplis M.J. et al. (2013) *M.A.P.S.*, 48, 2300-2315. [13] Elardo S.M. et al. (2012) *G.C.A.*, 87, 154-177. [14] Goodrich C.A. and Delaney J.S. (2000) *G.C.A.*, 64, 149-160. [15] Ghorso M.S. and Sack R.O. (1995) *Contributions of Mineralogy and Petrology*, 119, 197-212. [16] Chabot N.L. and Agee C.B. (2003) *G.C.A.*, 67, 2077-2091. [17] Pringle E.A. (2015) *EPSL*, 373, 75-82.